Correlations between pressure and bandwidth effects in metal–insulator transitions in manganites

Congwu Cui and Trevor A. Tyson[a)]
Physics Department, New Jersey Institute of Technology, Newark, New Jersey 07102

(Received 29 October 2003; accepted 9 December 2003)

The effect of pressure on the metal–insulator transition in manganites with a broad range of bandwidths is investigated. A critical pressure is found at which the metal–insulator transition temperature, T_{MI}, reaches a maximum value in every sample studied. The origin of this universal pressure and the relation between the pressure effect and the bandwidth on the metal–insulator transition are discussed. © *2004 American Institute of Physics.* [DOI: 10.1063/1.1646212]

Manganites have been the focus of intense studies in recent years since the observation of large magnetoresistance sparked interest in these materials for use as magnetoresistance sensors. The metal–insulator transitions (MITs) observed in these materials are crucial to the colossal magnetoresistance effect. MITs occur in manganites in two cases: First, a metallic ground state exists in the low-temperature range in some doping systems at certain doping concentrations, such as: $La_{1-x}Sr_xMnO_3$ ($x\sim0.16-0.50$), $La_{1-x}Ca_xMnO_3$ ($x\sim0.18-0.50$), and $Nd_{1-x}Sr_xMnO_3$ ($x\sim0.25-0.50$); second, metallic states can be induced by other factors, such as magnetic fields, photons, pressure, and electric fields. $Pr_{1-x}Ca_xMnO_3$ at $x\sim0.3$ is in the latter class. In most of the manganites, the metallic state is coupled to the ferromagnetic state so that the very large magnetoresistance can be explained by double exchange theory.

In the parameters determining the complicated properties of the manganites, the e_g electron bandwidth W is a particularly important one to the metal–transition temperature T_{MI}, or the appearance of the metallic state under some conditions. In manganites, the Mn $3d$ orbital is split into t_{2g} and e_g orbitals by the octahedral crystal field. The conduction-band electrons are of e_g symmetry. Because the e_g orbital is Jahn-Teller active for the Mn^{3+} sites, Jahn-Teller distortion (JTD) can further split the two-fold degenerate e_g orbital to trap the conduction-band electrons. Consequently, the bandwidth is highly correlated with the local atomic structure of the MnO_6 octahedra: Cooperative tilting (Mn—O—Mn bond angle), JTD (Mn—O distances), and coherence of the JTD. The bandwidth is characterized by the overlap between the Mn $3d$ orbital and O $2p$ orbital and can be described empirically by[1]

$$W\propto\frac{\cos\left[\frac{1}{2}(\pi-\langle\beta\rangle)\right]}{d_{\mathrm{Mn—O}}^{3.5}}, \tag{1}$$

where W is the bandwidth, β is the Mn—O—Mn bond angle, and $d_{\mathrm{Mn—O}}$ is the Mn—O bond length. In double exchange theory, it is described as the electron hopping rate or the transfer integral: $t_{ij}=t_{ij}^0\cos(\theta_{ij}/2)$, where t_{ij}^0 is the transfer integral that depends on the spatial wave function overlaps and θ_{ij} is the relative angle between two neighboring Mn ion t_{2g} core spins.

Generally, the structure can be tuned in two ways: Chemical doping and external pressure. In chemical doping, by selecting different doping elements and doping concentration, the average A-site atom size $\langle r_A\rangle$ in the $AMnO_3$ system is changed. Because of the mismatch between $\langle r_A\rangle$ and Mn-site ion size, the local atomic structure of MnO_6 octahedra can be modified. Therefore, the bandwidth is tuned by chemical doping so that complicated electronic and magnetic phase diagrams have been observed.[2] The external pressure method is a ''clean method'' that only modifies the lattice structure without inducing chemical complexity. To date, in studies on manganites, the effects of external pressure on the charge ordering, MITs, and magnetic states have been observed.

Currently, most of the high-pressure studies on manganites are on MITs and at low pressures ($\leqslant2$ GPa). In the low-pressure range, this electronic transition is coupled to the ferromagnetic transition, which can be explained qualitatively by double exchange theory.[3,4] It is also found that hydrostatic pressure has similar effects to chemical doping with larger atoms and higher doping concentration. Both can increase the Mn—O—Mn bond angle, compress Mn—O bond length and, hence, lead to larger bandwidth. Correspondingly, T_C (or T_{MI}) increases, or in some manganites originally in insulating state, a MIT is induced. The effect of chemical doping and pressure can be scaled to each other with a conversion factor of 3.75×10^{-4} Å/kbar.[5] However, most pressure experiments were conducted below 2 GPa.

By applying pressures up to ~6 GPa on manganite systems with a broad range of bandwidths, the effect of pressure on the MIT and the correlation between the external pressure effect and the chemical doping were observed. It is found that T_C and/or T_{MI} do not change monotonically with pressure[6] and these two transitions do not always couple.[7] A universal pressure may exist for the MIT in manganites. With an increase of the bandwidth, the change in the MIT temperature with pressure may vanish.

To systemically explore the external pressure and chemical doping effects and the correlation between them, manganite systems with much different ground magnetic and electronic states, $Nd_{1-x}Sr_xMnO_3$ ($x=0.45$, 0.50) (NSMO),

a)Electronic mail: tyson@adm.njit.edu

TABLE I. Average A-site ion size, tolerance factor, T_{MI}, dT_{MI}/dP, and critical pressure.

Sample	$\langle r_A \rangle$	t	T_{MI} (K)	dT_{MI}/dP (K/GPa)	P^* (GPa)
PCMO25	1.179 25	0.927 11	N/A[a]	51(7)	3.8(9)
PCMO30	1.179 30	0.928 30	N/A[a]	88(7)	3.5(4)
PCMO35	1.179 35	0.929 50	N/A[a]	68(7)	3.9(3)
LYCMO	1.202 30	0.937 30	149(1)	22(4)	3.8(4)
NSMO45	1.229 15	0.949 87	291(1)	18(11)	2.6(1.6)[b]
NSMO50	1.236 50	0.953 74	256(1)	−1.0(2.8)	3.0(1.6)

Note: t is the tolerance factor calculated with the data in Ref. 12, T_{MI} is the MIT temperature at ambient pressure, dT_{MI}/dP is the change rate of T_{MI} at $P\sim0$ extracted by fitting the data with a third-order polynomial, the numbers in brackets are the errors in the last one or two digits, and P^* is the pressure where the T_{MI} increase trend reverses.

[a]N/A denotes not applicable.

[b]The evolution of resistivity in the paramagnetic phase at ~316 K gives a P^* of 3.8±0.3 GPa. (See Ref. 9). See text for details.

$La_{0.60}Y_{0.07}Ca_{0.33}MnO_3$ (LYCMO), and $Pr_{1-x}Ca_xMnO_3$ ($x=0.25$, 0.30, 0.35) (PCMO), were selected. The bandwidths of the selected samples are uniformly distributed in the electronic phase diagram (see Ref. 5).

The samples were prepared by solid-state reaction. The procedure and details of preparation were described elsewhere.[6,8,9] All samples are characterized with x-ray diffraction and magnetization measurements. The details of the high-pressure resistivity measurement method and error analysis were described previously.[6] The MIT temperature whenever present is defined as the temperature at the resistivity peak. Because of the lower temperature stability of our system in the cooling cycle, the data were collected only while warming up.

In all the samples studied, there is a MIT at ambient pressure or a MIT can be induced by applying pressure. Corresponding to the bandwidth phase diagram in Ref. 5, the $Nd_{1-x}Sr_xMnO_3$ system ($x=0.45$, 0.50) has a large bandwidth, $La_{0.60}Y_{0.07}Ca_{0.33}MnO_3$ has a medium bandwidth, and the $Pr_{1-x}Ca_xMnO_3$ system ($x=0.25$, 0.30, 0.35) has a small bandwidth.

In Table I, $\langle r_A \rangle$, the tolerance factor t, and MIT temperature at ambient pressure, which corresponds to the bandwidth, are listed. The average Mn—O bond length and Mn—O—Mn bond angle of all samples determined from the Rietveld refinement to the x-ray diffraction patterns are shown in Fig. 1. According to Eq. (1), with increasing $\langle r_A \rangle$ or t, the decreasing bond length and bond angle lead to increasing bandwidth W and, hence, increasing T_{MI}.

With the application of pressure, the MIT temperatures of the samples which have a MIT at ambient pressure increase. In the narrow bandwidth $Pr_{1-x}Ca_xMnO_3$ system, the samples are insulating at ambient pressure. Under pressure, MITs are induced. With a pressure increase, the behavior of the T_{MI} is similar to other samples with a larger bandwidth. When the pressure is above a certain point, the increasing trend of T_{MI} of all samples is reversed. The evolution of the transition temperatures of all samples is shown in Fig. 2.

In Fig. 2, the most salient feature is that a critical pressure P^* exists in each sample: With a pressure increase, below P^*, T_{MI} increases; above P^*, T_{MI} decreases. By fitting T_{MI} versus P plots with a third-order polynomial, P^* for each sample can be extracted and is listed in Table I. Within the fitting error, the samples have the same critical pressure P^*. One exception is the NSMO45 sample. The P^* determined from the T_{MI} is small. But, if we look at the resistivity changes with pressure, its critical pressure is the same as other samples. This may come from the high-temperature limit of the instruments which leads to the fact that the T_{MI} near the limit in the middle pressure range cannot be determined.[9]

In large bandwidth samples, the change of T_{MI} with pressure is slower than in narrow bandwidth ones, indicating that the large bandwidth samples are more stable under pressure. The samples studied are selected with different doping concentrations and from different doping systems. The bandwidths span a large range. The samples also have rather different ground-state electronic and magnetic properties at ambient conditions. But, the MITs in these samples all follow a similar behavior, therefore, it is reasonable to speculate that the critical pressure P^* is universal for the MITs in manganites. From the structural measurements on manganites,[6,10,11] the behavior of T_{MI} under pressure could possibly be ascribed to a local atomic structure transformation of the MnO_6 octahedra.

Under pressure, the smaller bandwidth samples seem to a have smaller pressure range in which the samples are metallic at low temperature and outside which they are insulating. On the other hand, the samples with a large bandwidth

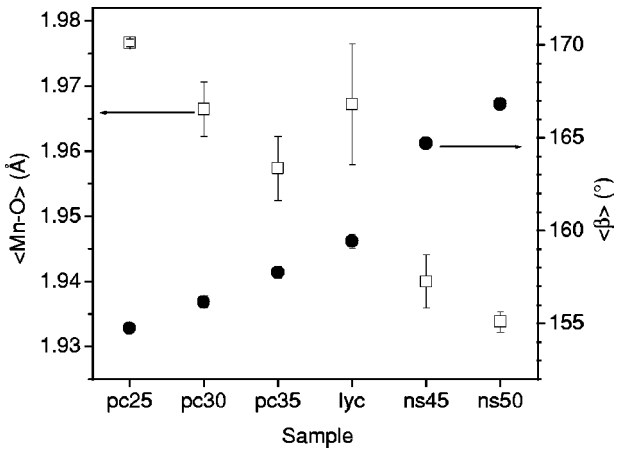

FIG. 1. Mn—O bond length and Mn—O—Mn bond angle of samples at ambient conditions. Note: The abscissa gives the samples, the numbers indicate the concentrations of the doping elements in percent; p represents Pr, c represents Ca, ℓ represents La, y represents Y, n represents Nd, and s represents Sr.

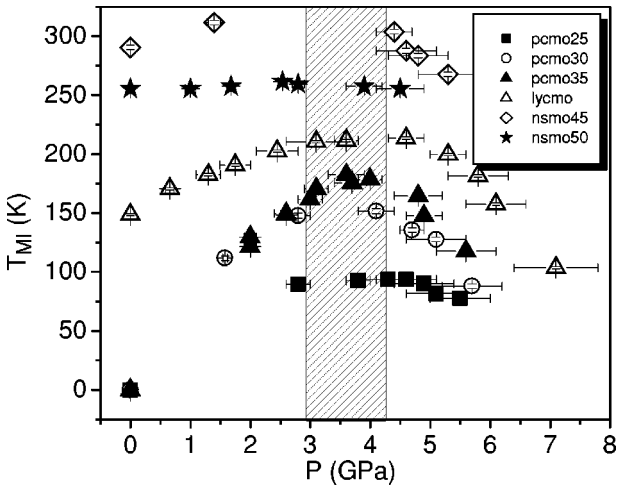

FIG. 2. Pressure dependence of the MIT temperatures of $Nd_{1-x}Sr_xMnO_3$ ($x=0.45$, 0.50), $La_{0.60}Y_{0.07}Ca_{0.33}MnO_3$, and $Pr_{1-x}Ca_xMnO_3$ ($x=0.25$, 0.30, 0.35).

are more stable under pressure and the variable range of T_{MI} is small, and they do not become insulating in a larger pressure range. The lower stability of T_{MI} in small bandwidth samples may come from the small A-site atoms, which leave more space between the octahedra for them to rotate—accordingly, a smaller pressure window for the metallic state.

In Fig. 2, the large bandwidth samples have higher MIT temperatures. The only exception is that in the $Nd_{1-x}Sr_xMnO_3$ system, the $x=0.5$ compound nominally has a larger bandwidth than the $x=0.45$ compound but has a lower T_{MI}. This possibly results from the strong charge ordering effect in $Nd_{0.5}Sr_{0.5}MnO_3$.

The rate of change of the MIT temperature with pressure at the ambient pressure, dT_{MI}/dP at $P=0$, is also interesting. The values of dT_{MI}/dP extracted from the third-order polynomial fitting results are listed in Table I. Clearly, the smaller the bandwidth, the larger dT_{MI}/dP, indicating that the local structure of the smaller bandwidth sample is more distorted and has a relatively large degree to which it can be compressed by pressure.

In summary, by applying external pressure on manganites of different chemical doping systems and doping concentrations and, hence, different e_g electron bandwidths, it is found that the pressure effect on the MIT in manganites is not equivalent to that of the chemical doping. Only at low pressures is the pressure effect on the MIT analogous to the chemical doping with elements of a large atom size. With a pressure increase, the trend of T_{MI} increasing with pressure is reversed at a critical pressure, above which the transition temperature decreases with pressure and, finally, the material may become insulating. The critical pressure is found to exist in all of the samples studied and possibly is universal for the MIT in the manganites. The bandwidth (chemical doping) determines how stable the material may be under pressure. The larger bandwidth manganites are more stable under pressure and, therefore, have a smaller dT_{MI}/dP near ambient pressure and smaller T_{MI} variation under pressure. Because of the importance of the local atomic structure of the MnO_6 octahedra to the electronic and magnetic properties of the manganites, this work may also contribute to understanding the properties of thin films of manganites which are important in technological applications.

This work is supported by the National Science Foundation under Grant No. DMR-0209243.

[1] M. Medarde, J. Mesot, P. Lacorre, S. Rosenkranz, P. Fischer, and K. Gobrecht, Phys. Rev. B **52**, 9248 (1995).
[2] Y. Tokura and Y. Tomioka, J. Magn. Magn. Mater. **200**, 1 (1999).
[3] J. J. Neumeier, M. F. Hundley, J. D. Thompson, and R. H. Heffner, Phys. Rev. B **52**, R7006 (1995).
[4] Y. Moritomo, H. Kuwahara, Y. Tomika, and Y. Tokura, Phys. Rev. B **55**, 7549 (1997).
[5] H. Y. Hwang, T. T. M. Palstra, S.-W. Cheong, and B. Batlogg, Phys. Rev. B **52**, 15046 (1995).
[6] C. Cui, T. A. Tyson, Z. Zhong, J. P. Carlo, and Y. Qin, Phys. Rev. B **67**, 104107 (2003).
[7] C. Cui and T. A. Tyson, Appl. Phys. Lett. **83**, 2856 (2003).
[8] C. Cui and T. A. Tyson (unpublished).
[9] C. Cui, T. A. Tyson, Z. Chen, and Z. Zhong, Phys. Rev. B **68**, 214417 (2003).
[10] A. Congeduti, P. Postorino, E. Carmagno, M. Nardone, A. Kumar, and D. D. Sharma, Phys. Rev. Lett. **86**, 1251 (2001).
[11] C. Meneghini, D. Levy, S. Mobilo, M. Ortolani, M. Nuñez-Reguero, A. Kumar, and D. D. Sharma, Phys. Rev. B **65**, 012111 (2002).
[12] R. D. Shannon and C. T. Prewitt, Acta Crystallogr., Sect. A: Cryst. Phys., Diffr., Theor. Gen. Crystallogr. **32**, 785 (1976).